Published in final edited form as:
Cancer Res. 2008 November 1; 68(21): 8705–8714. doi:10.1158/0008-5472.CAN-08-0923.

p37^{Ing1b} Regulates B-Cell Proliferation and Cooperates with p53 to Suppress Diffuse Large B-Cell Lymphomagenesis

Andrew H. Coles[1], **Concetta G.A. Marfella**[1], **Anthony N. Imbalzano**[1], **Heather A. Steinman**[1], **David S. Garlick**[2], **Rachel M. Gerstein**[3], and **Stephen N. Jones**[1,2]

[1]Department of Cell Biology, University of Massachusetts Medical School, Worcester, Massachusetts

[2]Department of Cancer Biology, University of Massachusetts Medical School, Worcester, Massachusetts

[3]Department of Molecular Genetics and Microbiology, University of Massachusetts Medical School, Worcester, Massachusetts

Abstract

The Inhibitor of Growth (ING) gene family encodes structurally related proteins that alter chromatin to regulate gene expression and cell growth. The initial member, ING1, has also been proposed to function as a tumor suppressor in human cancer based on its ability to suppress cell growth and transformation *in vitro*. Mouse *Ing1* produces two proteins (p31 and p37) from differentially spliced transcripts. We have recently generated p37^{Ing1b}-null mice and observed spontaneous follicular B-cell lymphomagenesis in this model to show that ING proteins can function *in vivo* as tumor suppressors. In this present report, we examine the role of p37^{Ing1b} in the regulation of B-cell growth and explore the relationship between p37^{Ing1b} and p53-mediated tumor suppression. Our results indicate that p37^{Ing1b} inhibits the proliferation of B cells and follicular B cells regardless of p53 status, and loss of p53 greatly accelerates the rate of B-cell lymphomagenesis in p37^{Ing1b}-null mice. However, in contrast to the highly penetrant follicular B-cell lymphomas observed in p37^{Ing1b}-null mice, mice lacking both p37^{Ing1b} and p53 typically present with aggressive diffuse large B-cell lymphomas (DLBL). Analysis of marker gene expression in p37^{Ing1b}/p53 null tumors indicates that the double-null mice develop both nongerminal center and germinal center B-cell–like DLBL, and also documents up-regulation of nuclear factor-κB activity in p37^{Ing1b}/p53-null B cells and B-cell tumors. These results confirm that p53 mutation is an important mechanistic step in the formation of diffuse large B-cell lymphomas and reveals a p53-independent role for Ing1b in suppressing B-cell tumorigenesis.

Introduction

Follicular B-cell lymphoma (FL) and diffuse large B-cell lymphoma (DLBL) account for approximately half of all malignant, non–Hodgkin lymphomas in adults (1–3). Patients with FL typically display microscopic accumulations (follicles) of CD45R/B220+ B cells in lymph nodes. The median survival time for FL patients is 8 to 10 years with a variable disease course that is usually protracted with multiple relapses after treatment (1,4). Eventually, the tumor

Requests for reprints: Stephen N. Jones, Department of Cell Biology, University of Massachusetts Medical School, 55 Lake Avenue North, Worcester, MA 01655. Phone: 508-856-7500; Fax: 508-856-7510; stephen.jones@umassmed.edu..

Disclosure of Potential Conflicts of Interest
No potential conflicts of interest were disclosed.

becomes resistant to chemotherapy and can undergo transformation to a more aggressive phase that is often fatal to the patient. In contrast, DLBL is a more aggressive type of lymphoma but with a more varied clinical course (5,6). Patients with DLBL display large, CD45R/B220+ lymphocytes in their tumor masses and a relatively high frequency of widespread organ involvement. DLBL can arise either *de novo* from mature germinal center (GC) B cells (GCB) or via transformation from a less aggressive B-cell lymphoma, such as FL (7). Although the disease responds initially to chemotherapy, a durable remission occurs in fewer than half of treated DLBL patients.

Several groups have used either cDNA microarrays or immunohistochemistry to divide DLBL into three subgroups with prognostic significance; GCB-like, activated B-cell–like (ABC), or type 3 expression profile (8,9). The expression of *CD10*, *BCL-6*, and *IRF-4* (*MUM1*) are used to differentiate the GCB from ABC subtypes. GCB-like DLBL usually expresses *CD10* but can also have a *CD10-*, *BCL-6+*, *IRF-4–* signature (10). This subgroup has the best prognosis with 60% of patients surviving for 5 years or more (11). ABC DLBL, also called non-GCB, can have several different expression signatures, such as *CD10–*, *BCL-6–*, or *CD10–*, *BCL-6+*, *IRF-4+*. ABC-DLBL has a less favorable prognosis with only ~35% of patients surviving to 5 years (11). The third subgroup of DLBL encompasses those cases that do not express genes characteristic of either the ABC or GCB types. It also has a poor prognosis similar to ABC-DLBL but is less well-studied (12).

Despite the morphologic heterogeneity of human B-cell lymphomas, a number of common genetic alterations have been observed. The most prevalent is a t(14;18) translocation seen in human FL, which results in *BCL-2* overexpression and protection of cells from apoptosis. Because the t(14:18) translocation is also detected in healthy human B cells, *Bcl-2* overexpression is thought to be necessary but not sufficient to induce FL. Furthermore, mice harboring an Eμ promoter-Bcl-2 transgene fail to develop spontaneous lymphoma (13), and overexpression of *BCL-2* is not observed in all human FL. These data suggest that an alternative prosurvival mechanism may exist in these tumors. In support of this finding, overexpression of *MCL-1* has also been detected in human B-cell lymphomas (14). MCL-1 is an antiapoptotic BCL-2 family member required for survival of both T and B cells (15), and MCL-1 transgenic mice develop widely disseminated B-cell lymphomas displaying a variety of histologic subtypes, including FL and DLBL (16). In addition, BCL-6, a critical regulator of the GC response wherein B-cells undergo antigen-driven somatic hypermutation to generate high affinity antibodies, is another prosurvival BCL-2 family member often dysregulated in B-cell lymphoma. Chromosomal translocations involving *BCL-6* have been observed in 15% to 40% of human DLBL and 5 to 10% of FL cases (17), and transgenic mice expressing exogenous *Bcl-6* in B-cells developed a GCB-like subtype of DLBL (18). Collectively, these findings support a role for overexpression of various BCL-2 family members in the pathogenesis of B-cell lymphomas.

Mutations in the p53 tumor suppressor gene have been observed in many types of human lymphomas and often correlate with a poor patient prognosis. Furthermore, mutations in p53 have been proposed to play a role in the transformation of FL to a more aggressive DLBL (19–21). However, recent work suggests that p53 may have a limited role in the transformation of FL to DLBL (22), and mice either deficient for p53 or bearing a transgene encoding the p53-inhibitor Mdm2 do not develop FL or DLBL. Rather, these mouse models develop CD4+/CD8+ T-cell lymphomas, B220+ marginal zone B-cell lymphomas, or mixed lineage T-cell and B-cell lymphomas (23–26). Thus, the precise role of p53 in suppressing the formation or transformation of FL and DLBL is unclear.

Recently, studies of Ing1-mutated mice have revealed a role for Inhibitor of Growth (ING) proteins in suppressing B-cell lymphomagenesis (27,28). ING1, a member of the ING gene

family, has been proposed to regulate a number of biological processes, including nucleotide excision repair, chromatin remodeling, proliferation, apoptosis, and senescence (29). In addition, ING1 has been proposed to function as a tumor suppressor by regulating p53 activity (29–32). Mouse *Ing1* encodes two different proteins (p31 and p37) from differentially spliced transcripts (33). Approximately 20% of mice lacking both p31 and p37 Ing1 proteins developed a B220+, B-cell lymphoma by age 23 months (28). A small percentage of these tumors were biphenotypic, expressed both B220 and CD3 surface antigens, and were classified as follicular (FO) center B-cell lymphomas (28). We have previously generated mice deficient solely for $p37^{Ing1b}$, the most prevalent isoform of Ing1. These mice developed spontaneous FO B220+ lymphomas between ages 1 and 2 years, and analysis of the growth and response of $p37^{Ing1b}$-deficient mouse embryonic fibroblasts (MEF) and thymocytes to DNA damaging agents revealed that $p37^{Ing1b}$ inhibited MEF proliferation and suppressed thymocyte apoptosis in a p53-independent manner (27). In the present study, we examined the role of $p37^{Ing1b}$ in B-cell growth and apoptosis, and explore the relationship between $p37^{Ing1b}$ and p53 in tumor suppression. Our data indicate that $p37^{Ing1b}$ inhibits FO B cell proliferation regardless of p53 status and that $p37^{Ing1b}$ and p53 cooperate to suppress the formation of non-GC and GCB-like DLBL. In addition, we find that nuclear factor-κB (NF-κB) activity is up-regulated in the absence of $p37^{Ing1b}$, supporting a role for mouse $p37^{Ing1b}$ in regulating NF-κB signaling. These results reveal a p53-independent role for $p37^{Ing1b}$ in suppressing B-cell lymphomagenesis and show that p53 deletion facilitates the formation of DLBL in a mouse model of FL.

Materials and Methods

Mice and tumor assay

The generation of $p37^{Ing1b}$-null mice and p37/p53-double null mice was described previously (27). The $p37^{Ing1b}$-null mice were backcrossed to C57Bl/6 strain for six generations, and cohorts of these mice and of p37/p53-double null mice, wild-type (wt) mice, and p53-null mice (34) all on a C57Bl/6 inbred background were collected and aged to perform a tumor assay. Mice displaying obvious tumors or signs of reduced vitality were euthanized and tissues were harvested for fluorescence-activated cell sorting (FACS) analysis or fixed in 10% formalin for immunohistochemistry. Samples were also flash frozen in liquid nitrogen for use in quantitative reverse transcription-PCR (qRT-PCR) analysis. Formalin fixed, paraffin-embedded sections were stained with either H&E or with an antibody to CD45R/B220 (BD PharMingen; 1:50) or to Bcl-6 (Santa Cuz; 1:50) before being analyzed by microscopy. All mice were maintained and used in accordance with both federal guidelines and those established by the Institutional Animal Care and Use Committee at the University of Massachusetts Medical School.

Cell sorting

Single cell suspensions of spleens harvested from p37/p53 double null mice at ages 6 to 8 wk were stained with CD45R/B220-PE (eBiosciences; 1:200) or IgD-PE (eBiosciences; 1:200) and FACS sorted. Resulting purity of either total B-cell (B220+) or FO B-cell (IgD^{Hi}) populations were >95%. B-cells were maintained in RPMI 1640 supplemented with 5% FCS, 2 mmol/L L-glutanine, 100 μg/mL streptomycin, 100 U/mL penicillin, and 50 μmol/L 2-mercaptoethanol (Life Technologies-Bethesda Research Laboratories) and cultured at 37°C and 10% CO_2. Double positive (DP) thymocytes were sorted using CD4-PE (BD PharMingen; 1:250) and CD8-APC (BD PharMingen; 1:100) antibodies and sorted by FACS. RNA from sorted DP T-cells was purified using Trizol reagent from Invitrogen according to the manufacturer's instructions, and cDNA was generated using a first-strand cDNA synthesis kit from Invitrogen.

Analysis of B-cell subsets

Spleens were processed to single-cell suspension by pressing between frosted glass slides, and filtered through nylon mesh. RBC were lysed using brief hypotonic shock and the remaining cells were resuspended in biotin-, flavin-, and phenol red–deficient RPMI 1640 (Invitrogen) staining medium containing 10 mmol/L Hepes (pH 7.2), 0.02% sodium azide, 1 mmol/L EDTA, 3% newborn calf serum, and treated 10 min on ice with 2.4G2 Fc block (BD Biosciences). Cells were incubated for 20 min on ice with primary antibodies, washed, and biotin-stained cells were incubated with streptavidin-pacific blue (Molecular Probes/Invitrogen) for 15 min on ice. After two washes, cells were resuspended in 1 mg/mL propidium-iodide to exclude dead cells. Primary antibodies included antibodies specific for: CD24 (clone 30-F1) FITC or PE, CD45R/B220 (RA3-6B2) APC, IgM (II/41) biotin or FITC, IgD (11–26) PE, CD93/AA4.1 APC, and CD23 (B3B4) biotin. All reagents except when noted were from BD Biosciences, eBiosciences, Southern Biotechnology Associates, Inc., or CALTAG Laboratories/Invitrogen. Flow cytometry was performed on a 3-laser 12-color LSR II (BD Biosciences) and analyzed with FlowJo software (Tree Star).

Proliferation and apoptosis assays

Incorporation of [^{3}H] thymidine was used as a measure of proliferation as described previously (35). In brief, sorted 2×10^5 B cells were plated into wells of a 96-well plate with 200 μL of RPMI. After 24 h of culture, cells were pulsed with [^{3}H] thymidine (1 μCi per well) for 16 h before harvest. Incorporated radioactivity was quantified with a Liquid Scintillation and Luminescence Counter (Perkin-Elmer Wallace, Inc.). Apoptosis assays were described previously (36). In brief, B-cells were plated as before and then treated with either increasing amounts of anti-IgM F(ab')$_2$ (Jackson Immunoresearch), 250 rads γ-irradiation, 100 nmol/L dexamethasone (Sigma), or allowed to die by neglect. After 24 h after IR or 100 nmol/L dexamethasone treatment or 16 h after IgM treatment, cells were collected, stained for propidium iodide, and analyzed by FACS. Additionally, mice were treated with 10Gy IR and spleens were harvested 8 h later. Single-cell suspensions of splenocytes were stained with B220, Annexin V, and 7-AAD to measure apoptosis as previously described (36).

qRT-PCR

QRT-PCR was done as previously described (37). The primers used were as follows: *Mcl-1*, AGTCAGCACAGCTTTCCTGTCAGA and TGCCAATCCAAGAATGCCAATCCC; *Bcl-2*, CTCGTCGCTACCGTCGTGACTTCG and GTGGCCCAGGTATGCACCCAG; *Bcl-6*, GCAACGAATGTGACTGCCGTTTCT and TTTCTCACCCGTGTGGACAGTCTT; *CD10*, TTCTGTGGCCAGACTGATTCGTCA and GCAGCATTGGGTCATTTCGGTCTT; *Irf4*, GAGCTGCAAGTGTTTGCTCACCAT and ACAGTTGTCTGGCTAGCAGAGGTT; *RelA (p65)*, TGTGTTGATAGCTCCTGCTTCGGT and ATCAAGGTGTACAGGAATCCGCGT; *Il-6*, AGTCACAGAAGGAGTGGCTAAGGA and TCTGACCACAGTGAGGAATGTCCA; and *Ef1α*, AGCTTCTCTGACTACCCTCCACTT and GACCGTTCTTCCACCACTGATT. All primers were amplified using 62°C for an annealing temperature and 24 cycles to keep the products in the linear range. PCR products were run on a 2% agarose gel with SYBR green to visualize the bands.

Results

Mice deficient for p37^{Ing1b} have an expanded FO B-cell compartment

To characterize the B-cell compartment in p37^{Ing1b}-deficient mice, single-cell suspensions were prepared from spleens isolated from 6-month-old, asymptomatic mice and FACS analysis was performed. CD45R/B220 staining revealed a subtle expansion of splenic B-cell lymphocytes in p37^{Ing1b} null mice compared with age-matched wt mice (51.4% versus 36%

in wt), with a majority of the B220+ cells also staining positive for both IgM and CD23, a marker of FO cells (Fig. 1*A*). These data suggest that loss of $p37^{Ing1b}$ leads to an increase in the number of mature FO B cells in adult mice, consistent with a role for $p37^{Ing1b}$ in regulating the growth of these cells. Spleens harvested from mice deleted for both $p37^{Ing1b}$ and p53 revealed a similar expansion of these mature B cells (data not shown).

Proliferation, but not apoptosis, is altered in $p37^{Ing1b}$ and p37/p53 deficient B cells

To further investigate the role of $p37^{Ing1b}$ in B-cell growth, we isolated either total CD45R/B220+ B cells or FO (IgD^{hi}) B cells from the spleens of adult wt, $p37^{Ing1b}$-null, p53-null, and p37/p53-double null mice by FACS sorting using either anti-B220 or IgD-PE antibodies. Because anti-IgM $F(ab')_2$ antibodies activate B cells by cross-linking of the B-cell receptor complex (BCR) to initiate cell proliferation and death, we treated either total B cells or FO B cells with increasing amounts of anti-IgM antibody for 16 hours and measured cell proliferation via [^{3}H] thymidine incorporation (Fig. 1*B* and *C*). Both total B cells (Fig. 1*B*, *top*) and FO B cells (Fig. 1*C*, *top*) isolated from $p37^{Ing1b}$-deficient mice displayed increased proliferation relative to their wt counterparts. Although deletion of p53 also increased the proliferative response of FO B cells, codeletion of both $p37^{Ing1b}$ and p53 further increased the proliferation of the IgD^{hi}, FO B cells in response to BCR activation. As FO B cells from p37/p53-double null mice displayed even greater proliferation than observed in either p37-null or p53-null cells, these data indicate that $p37^{Ing1b}$ does not require functional p53 to inhibit FO B cell growth. Rather, the p37 and p53 tumor suppressors cooperate in negatively regulating the proliferation of these cells.

To confirm that the increased numbers of FO B cells observed both *in vivo* in p37 ^{Ing1b}-null mice and in the *in vitro* proliferation assays were due to increased cell proliferation and not a reflection of altered cell death, we examined apoptosis in p37 ^{Ing1b}-null cells. Wt or $p37^{Ing1b}$-null mice were mock treated or exposed to 10 Gy ionizing radiation. Eight hours after IR treatment, single-cell suspensions of splenocytes were prepared from the mice and stained with B220, Annexin V, and 7-AAD to determine the percent of cells undergoing apoptosis. No difference in cell death was observed between wt and $p37^{Ing1b}$-null splenocytes, as measured by depletion of B220+ cells or by increased Annexin V + staining (Fig. 1*B*, *middle*). To confirm these *in vivo* results, total B-cells (B220+) and FO B-cells (IgD^{hi}) were isolated from the spleens of adult wt, $p37^{Ing1b}$-null, p53-null, and p37/p53-double null mice and grown in prolonged culture or treated with increasing amounts of anti-IgM or dexamethasone to induce cell death. Sub-G_1 content after staining of the B220+ or IgD^{hi} cells with propidium iodide was used to identify the percentage of apoptotic cells in each population (Fig. 1*B*, *bottom*; Fig. 1*C*, *middle* and *bottom*). Although prolonged culture *in vitro* or activation of BCR by anti-IgM treatment increased apoptosis in FO B cells, the presence or absence of $p37^{Ing1b}$ did not alter the apoptotic response of the FO B cells. In addition, there was no difference in the apoptotic response of wt, p37 ^{Ing1b}-null, p53-null, or p37/p53-double null FO B-cells to treatment *in vitro* with either 2.5 Gy ionizing radiation or with 100 nmol/L dexamethasone (data not shown). Thus, although $p37^{Ing1b}$ does alter apoptosis in total B cells when treated with dexamethasone, a p53-independent inducer of cell death, $p37^{Ing1b}$ does not seem to play a role in regulating apoptosis in FO B cells in response to these stimuli. The FO B-cell data contrast with the increased apoptosis we observed previously in $p37^{Ing1b}$-null thymocytes (27), and confirm that the increase in FO B-cell numbers observed in adult p37 ^{Ing1b}-null mice is likely due to increased proliferation of these cells.

p37/p53 double null mice primarily develop aggressive B-cell lymphomas

The increase in FO B-cell proliferation when codeleted for $p37^{Ing1b}$ and p53 suggests that $p37^{Ing1b}$ and p53 may cooperate to suppress B-cell tumorigenesis. To test this hypothesis, we collected cohorts of wt mice, $p37^{Ing1b}$-null mice, p53-null mice, and p37/p53 double-null mice

and compared the rate of spontaneous tumor formation (Fig. 2*A*) and the spectrum of tumor types (Fig. 2*B*) in these mice. The $p37^{Ing1b}$-null mice presented with FL between ages 1 and 2 years, in agreement with our previous report (27). Three quarters of the $p37^{Ing1b}$-null cohort developed spontaneous cancer, whereas wt mice did not develop tumors during this time. Tumors arising in $p37^{Ing1b}$-null mice were predominantly localized to the lymph or spleen, with little or no involvement of peripheral tissues. As expected, all p53-null mice succumbed to spontaneous tumorigenesis within 10 months, with 75% of the tumors classified as lymphomas and the remainder a mix of sarcomas and carcinomas. As previously reported, two-thirds of the p53-null lymphomas formed in the thymus and were composed of CD4+CD8+ T cells, whereas the remaining third of the lymphomas formed in the spleen and were classified as marginal zone B-cell lymphomas or as polymorphic tumors containing both B cells and T cells (23–25,34,38). Similarly, p53-null mice codeleted for p37 rapidly formed spontaneous tumors by age 45 weeks (Fig. 2*A*). However, all of the p37/p53-double null mice presented with lymphoma, with three quarters (17/23) of the p37/p53-null mice displaying enlarged spleens, discolored and enlarged livers, and lymph node involvement. Microscopic analysis of H&E-stained tumor samples isolated from p37/p53-double-null mice revealed evidence of a lymphoblastic lymphoma involving spleen, liver, and/or mesenteric lymph node (Fig. 3*A*). In contrast to tumorigenesis in p53-null mice, only a small subset (6 of 23) of lymphomas arising in p37/p53-double null mice formed in the thymus (Fig. 2*B*).

The nonthymic p37/p53-double null tumors were characterized by a uniform population of large, malignant lymphocytes with round, vesicular nuclei with frequent membrane indentations, occasional centrally placed nucleoli, and scanty cytoplasm. Lymphoblasts completely effaced lymph node architecture, diffusely involved the splenic white pulp, and infiltrated periportal and sinusoidal regions in the liver. Immunohistochemistry performed on select sections of paraffin-embedded tumors isolated from $p37^{Ing1b}$ mice and from p37/p53-double null mice using antibodies against CD45R/B220 and CD3 antigens confirmed that the predominant tumor type was a CD45R/B220+ lymphoma (data not shown; Fig. 3*A*). As multiple sites within the same p37/p53-double null mouse contained tumor nodules, in contrast to the typical single site in p37-null mice, and because p37/p53-double null mice present tumors faster and die much earlier than p37-null mice, deletion of both tumor suppressor genes seems to lead to the formation of a more aggressive B-cell tumor.

Although deletion of p53 greatly accelerated tumorigenesis in $p37^{Ing1b}$-null mice ($P < 0.05$), codeletion of $p37^{Ing1b}$ and p53 seemed to also delay slightly tumor onset in p53-null mice (Fig. 2*A*), although the difference in the tumor curves was subtle ($P < 0.1$). This may reflect the reduced incidence in p37/p53-double null mice of the highly aggressive thymic lymphomas typically seen in p53-null mice (Fig. 2*B*). Furthermore, the cellular characteristics of the thymic lymphomas arising in the p37/p53-double null mice seemed different from those arising in p53-null mice. FACS analysis of thymii isolated from p53-null and p37/p53-double null mice revealed that the CD4+CD8+ population was somewhat larger in p37/p53-double null mice relative to p53-null mice (Fig. 3*C*). Analysis of a thymic tumor originating in p37/p53-double null mice revealed an expansion of the non-CD4+CD8+ compartments. In contrast, FACS analysis of p53-null thymic tumors indicated that these tumors originated in CD4+/8+ DP T-cell compartment (Fig. 3*C*), in agreement with earlier studies (25).

We previously reported that thymocytes lacking $p37^{Ing1b}$ display up-regulated levels of proapoptotic *Bax* expression and possess an increased susceptibility to cell death induced by various stimuli (27). To confirm that the $p37^{Ing1b}$ null CD4+CD8+ cells codeleted for p53 also have increased *Bax* expression, we isolated total RNA from CD4+CD8+ thymocytes harvested from p37/p53-double null mice and performed qPCR to measure *Bax* transcripts. A modest increase in *Bax* mRNA (1.26 ± 0.02) was observed relative to wt CD4+CD8+ *Bax* transcript levels (Fig. 3*D*). The increase in *Bax* expression in p37/p53-double null CD4+CD8+ cells

correlates with the decrease incidence of CD4+CD8+ thymic lymphomagenesis observed in the double null mice and may account for the overall slight delay in the rate of tumorigenesis in p53-null mice codeleted for $p37^{Ing1b}$.

DLBL in p37/p53 double null mice

FACS analysis was performed on the B-cell compartments of two tumor-bearing mice to further characterize the tumor phenotype of the p37/p53-double null mice (Fig. 4*A*). Several distinct splenic B-cell populations were readily observed in nontumor-bearing mice, including FO B cells (IgD^{++} IgM^{lo} $CD23^{+}$), immature T1 (IgD^{lo} IgM^{++} $CD23^{-}$) and T2 (IgD^{lo} IgM^{++} $CD23^{+}$ $CD24^{++}$ $AA4.1^{++}$) B cells. However, the splenic B cells of tumor-bearing p37/p53-double null mice were almost exclusively composed of FO B cells (IgD^{++} IgM^{lo} $CD23^{+}$ $CD24^{lo}$ $AA4.1^{-}$). In addition, the forward scatter distribution of this FO B population is shifted (Fig. 4*A*, *right*), indicating that the majority of the FO B cells are larger, blast stage cells rather than resting cells. The phenotype of FO B cells in p37/p53 tumorigenic mice was distinguished by elevated levels of IgM and CD23 staining, and reduced amounts of CD24 staining relative to levels observed in wt FO B cells (Fig. 4*A*). Similar results were obtained in a repeat of this experiment (data not shown). The difference in the staining patterns of the $p37^{Ing1b}$-null tumor cells and p37/p53-double null tumor cells, coupled with the widespread organ involvement and larger size of the tumor cells arising in p37/p53-double null mice, classifies these CD45R/B220+ tumors as DLBL rather than FL.

To determine if there was increased expression of prosurvival genes in lymphomas arising in the double null mice as had been previously observed in human FL and DLBL (11,13,39), real-time PCR was performed on total RNA isolated from the spleens and tumors of various mice. *Mcl-1* expression seemed unaltered in wt, $p37^{Ing1b}$-null, and in p53-null cells but was slightly up-regulated in p37/p53 double-null spleens (Fig. 4*B*). However, *Mcl-1* expression levels were greatly increased in tumors arising in p37/p53-double null mice. In contrast, *Bcl-2* was not elevated in splenic tissues or in tumors, regardless of the genotype of the mice.

Approximately one-third of all NHL display translocations involving BCL-6, a transcriptional repressor required for the formation of GCB cells. Overexpression of BCL-6 has been proposed to block the terminal differentiation of GC B cells by inhibiting the expression of the B lymphocyte maturation protein 1, resulting in prolonged exposure of the GC B cells to the mutagenic effects of the somatic hypermutation machinery (40). In addition, Bcl-6 has been proposed to suppress DNA damage-induced apoptosis caused by the hypermutation apparatus by suppressing p53 expression (41). Thus, Bcl-6 expression serves as a marker for DLBL that are derived from GC-like B cells. To determine if *Bcl-6* expression was up-regulated in DLBL in p37/p53-double null mice, representative tissue sections were fixed, sectioned, and stained for Bcl-6 (Fig. 3*B*). Bcl-6 was not detected in wt tissue, or in a B-cell lymphoma arising in the spleen of a p53-null mouse (Fig. 3*B*). In contrast, varying levels of Bcl-6 expression could be detected in some but not all tumor tissues harvested from p37/p53-double null mice (Fig. 3*B*). To confirm up-regulation of *Bcl-6* expression in a subset of p37/p53-tumors, total RNA was harvested from 13 p37/p53-double null DLBL and assayed for *Bcl-6* transcript levels by qRT-PCR. In addition, the expression levels of the *CD10* surface marker, *Irf-4* transcription factor, and the NF-κB subunit *Rela (p65)* were also assayed by qRT-PCR (Table 1). Irf-4 is a transcription cofactor expressed in plasma cells that silences BCL-6 expression and the GC transcriptional program, and is critical for GC to plasma cell differentiation (42). *Bcl-6* was up-regulated in 6 of 13 tested DLBL that arose in p37/p53-double null mice, marking these tumors as GCB-like DLBL. CD10, another marker for GCB (43), was elevated in two other tumors, indicating that 8 of the 13 tumors were the GC subtype of DLBL. The remaining 5 DLBL tumors did not display elevated levels of *CD10*, *Bcl-6*, or *Irf-4*. Lack of *CD10*, *Bcl-6*,

or *Irf-4* up-regulation in the remaining five DLBL indicates that these are non–GCB-like DLBL tumors.

NF-κB activity is often increased in human lymphomas due to chromosomal translocations, mutation of NF-κB inhibitors such as IκB, or through other, less well-characterized processes (44,45). Furthermore, NF-κB activation is also observed in subtypes of non-GC DLBL such as in peripheral (or activated) B cell–like DLBL. Recently, the ING1 protein has been proposed to inhibit NF-κB signaling in human fibroblasts by up-regulating *HSP70* expression (46). To examine NF-κB activity in cells deleted for $p37^{Ing1b}$, qPCR was performed on total RNA isolated from the 13 DLBL samples. Analysis of *RelA* expression levels in the DLBL revealed that the *RelA (p65)* subunit expression was elevated in nearly all of the tumors (Table 1, *right column*) relative to *RelA* expression in wt splenic tisssue. To determine if NF-κB activity is up-regulated in p37/p53-double null cells, FO B cells were isolated from the spleens of wt, $p37^{Ing1b}$-null, p53-null, or p37/p53 double-null mice, and cell proliferation was measured in response to treatment of the cells with lipopolysaccharide (LPS), an established inducer of NF-κB activity (Fig. 5*A*). Although deletion of p53 or $p37^{Ing1b}$ did not result in a greater proliferative response of FO B cells to LPS, codeletion of p53 and $p37^{Ing1b}$ did result in increased proliferation of FO B cells to varying dosages of LPS. To confirm that the increase in *RelA* expression observed in the DLBL samples correlated with increased NF-κB activity in the tumors, qPCR was used to measure expression of the Interleukin 6 gene (IL-6), a classic target gene up-regulated by NF-κB signaling (Fig. 5*B*). Increased *IL-6* transcript levels were observed in the spleens of p37-null mice, regardless of p53 status, and very large increases (100- to 600-fold) in *IL-6* expression levels were observed in p37/p53 double-null tumors, regardless of their classification as GCB-like DLBL (tumor #5 and #7) or as non-GC DLBL (tumor #9 and #11). These results confirm that loss of $p37^{Ing1b}$ up-regulates NF-κB activity in p37/p53 double-null mice and in tumors, supporting a role for $p37^{Ing1b}$ in inhibiting NF-κB signaling in suppression of DLBL.

Discussion

We have previously described the generation of mice deleted for the $p37^{Ing1b}$ isoform of Ing1 (27). Loss of $p37^{Ing1b}$ increased the proliferation of MEF regardless of p53 status, and the p53-mediated response of cells to DNA damage or to overexpression of oncogenic *Ras* was unaltered in $p37^{Ing1b}$ deficient MEFs. In addition, deletion of $p37^{Ing1b}$ up-regulated *Bax* gene expression in the presence or absence of functional p53, and increased the apoptotic response of thymocytes to DNA damage. A majority of $p37^{Ing1b}$-deficient mice spontaneously developed enlarged spleens between ages 1 and 2 years. Histopathology revealed a CD45R/B220+ CD3– lymphocytic hypercellularity in spleens isolated from $p37^{Ing1b}$-deficient mice, and all of the tumors arising in $p37^{Ing1b}$-null mice were classified as FL (27). Although our results indicated that $p37^{Ing1b}$ can inhibit cell growth and cell death in a p53-independent manner, in MEFs and in thymocytes, respectively, it was unclear from these data if $p37^{Ing1b}$ alters p53 functions to regulate tumorigenesis. In this present study, we crossed $p37^{Ing1b}$ mice with p53-null mice to generate p37/p53-double null mice and explored the relationship between $p37^{Ing1b}$ and p53 tumor suppression. Deletion of p53 greatly accelerated the rate of tumor formation in $p37^{Ing1b}$-null mice, an unexpected finding if $p37^{Ing1b}$ and p53 were functionally redundant, or if $p37^{Ing1b}$ suppressed tumorigenesis by signaling through p53. Thus, cooperation observed between the two tumor suppressors in preventing B-cell lymphomagenesis indicates that $p37^{Ing1b}$ does not suppress tumors by activating p53. Cooperation between $p37^{Ing1b}$ and p53 in tumor suppression is also in agreement with the increased rate of cell proliferation in FO B cells when codeleted for $p37^{Ing1b}$ and p53.

Interestingly, there was a reduction in the incidence of thymic lymphomas in the p37/p53-double null mice relative to the high incidence CD4+CD8+ thymomas in p53-null mice. This

reduction correlates with an increase in proapoptotic *Bax* expression observed in CD4+CD8+ T cells isolated from p37/p53-double null mice, in keeping with our previous finding of a dramatic increase in *Bax* mRNA in total thymus when treated with γ-irradiation (27). The reduced incidence of thymic lymphoma, typically an aggressive cancer resulting in rapid morbidity and mortality in p53-null mice, may account for the slight delay in the lethality of the p37/p53-double null mice. We also observed a slight decrease in expression of *Mcl-1* in thymii from p37/p53-null mice (data not shown). The elevation of *Mcl-1* in p37/p53-null spleens and reduction of *Mcl-1* in T cells might also explain the shift from a predominately T-cell lymphoma in p53-null mice to a more B-cell lymphoma in p37/p53-null mice. Approximately half of the tested DLBL were found to have elevated *Bcl-6* expression levels and/or increased *CD10* expression, indicating a GCB-like subtype of DLBL. In addition, nearly all of the tumors displayed elevated *RelA* expression and, in some cases, increased NF-κB activity. It is yet unclear how $p37^{Ing1b}$ is regulating the expression of *Bcl-6*, *CD10*, or *RelA* in DLBL, or the expression of *Mcl-1* and *Bax* in B and T cells. Further experimentation is needed to determine if this effect is indirect or is a direct effect of altered factor binding at the promoters of these genes.

A few studies have examined the expression of *ING1* in human primary hematopoetic malignancies and found no mutation of ING1 or alterations in *ING1* expression in myeloid leukemias (28,47–49). However, down-regulation of *ING1* expression has been reported in human mantle cell lymphomas in both primary tumors and cell lines (48,49). In addition, expression of *ING1* seems to be down-regulated in gene expression profiling data performed on human DLBL samples, although the reduction in *ING1* expression was not enough to highlight ING1 as a prognostic indicator for the disease in these studies (8,9). However, the results of our analysis of $p37^{Ing1b}$-deficient mice indicate that loss of $p37^{Ing1b}$ induces the highly penetrant formation of spontaneous FL and DLBL in mice, especially in mice codeleted for p53. Thus, the role of $p37^{Ing1b}$ in suppressing human B-cell lymphomas, especially DLBL, should be evaluated further.

Acknowledgments

Grant support: NIH grants RO1AI43534 (R. M. Gerstein) and RO1CA77735 (S. N. Jones).

We thank the University of Massachusetts Medical School (UMMS) Morphology Core for assistance with tissue preparation, Erin Cloherty, Richard Konz, and the UMMS Flow Cytometry Core for help with FACS analyses, Charlene Baron for assistance with manuscript figure preparation, and Huiling Liang for advice and helpful discussions. Core facilities used in this study were supported in part by Program Project grant P30DK32529 from the National Institute of Diabetes and Digestive and Kidney Diseases.

References

1. Hiddemann W, Buske C, Dreyling M, Weigert O, Lenz G, Unterhalt M. Current management of follicular lymphomas. Br J Haematol 2007;136:191–202. [PubMed: 17073892]
2. Lichtman MA. Battling the hematological malignancies: the 200 years' war. Oncologist 2008;13:126–38. [PubMed: 18305057]
3. Ng AK. Diffuse large B-cell lymphoma. Semin Radiat Oncol 2007;17:169–75. [PubMed: 17591563]
4. Hiddemann W, Unterhalt M. Current treatment strategies in follicular lymphomas. Ann Oncol 2006;17 (Suppl 10):x155–9. [PubMed: 17018716]
5. Hunt KE, Reichard KK. Diffuse large B-cell lymphoma. Arch Pathol Lab Med 2008;132:118–24. [PubMed: 18181663]
6. Abramson JS, Shipp MA. Advances in the biology and therapy of diffuse large B-cell lymphoma: moving toward a molecularly targeted approach. Blood 2005;106:1164–74. [PubMed: 15855278]
7. Armitage JO. How I treat patients with diffuse large B-cell lymphoma. Blood 2007;110:29–36. [PubMed: 17360935]

8. Monti S, Savage KJ, Kutok JL, et al. Molecular profiling of diffuse large B-cell lymphoma identifies robust subtypes including one characterized by host inflammatory response. Blood 2005;105:1851–61. [PubMed: 15550490]
9. Alizadeh AA, Eisen MB, Davis RE, et al. Distinct types of diffuse large B-cell lymphoma identified by gene expression profiling. Nature 2000;403:503–11. [PubMed: 10676951]
10. Hans CP, Weisenburger DD, Greiner TC, et al. Confirmation of the molecular classification of diffuse large B-cell lymphoma by immunohistochemistry using atissue microarray. Blood 2004;103:275–82. [PubMed: 14504078]
11. Lossos IS, Morgensztern D. Prognostic biomarkers in diffuse large B-cell lymphoma. J Clin Oncol 2006;24:995–1007. [PubMed: 16418498]
12. De Paepe P, De Wolf-Peeters C. Diffuse large B-cell lymphoma: a heterogeneous group of non-Hodgkin lymphomas comprising several distinct clinicopathological entities. Leukemia 2007;21:37–43. [PubMed: 17039226]
13. Bende RJ, Smit LA, van Noesel CJ. Molecular pathways in follicular lymphoma. Leukemia 2007;21:18–29. [PubMed: 17039231]
14. Michels J, Foria V, Mead B, et al. Immunohistochemical analysis of the antiapoptotic Mcl-1 and Bcl-2 proteins in follicular lymphoma. Br J Haematol 2006;132:743–6. [PubMed: 16487175]
15. Opferman JT, Letai A, Beard C, Sorcinelli MD, Ong CC, Korsmeyer SJ. Development and maintenance of B and T lymphocytes requires antiapoptotic MCL-1. Nature 2003;426:671–6. [PubMed: 14668867]
16. Zhou P, Levy NB, Xie H, et al. MCL1 transgenic mice exhibit a high incidence of B-cell lymphoma manifested as a spectrum of histologic subtypes. Blood 2001;97:3902–9. [PubMed: 11389033]
17. Saito M, Gao J, Basso K, et al. A signaling pathway mediating downregulation of BCL6 in germinal center B cells is blocked by BCL6 gene alterations in B cell lymphoma. Cancer Cell 2007;12:280–92. [PubMed: 17785208]
18. Cattoretti G, Pasqualucci L, Ballon G, et al. Deregulated BCL6 expression recapitulates the pathogenesis of human diffuse large B cell lymphomas in mice. Cancer Cell 2005;7:445–55. [PubMed: 15894265]
19. Ichikawa A, Kinoshita T, Watanabe T, et al. Mutations of the p53 gene as a prognostic factor in aggressive B-cell lymphoma. N Engl J Med 1997;337:529–34. [PubMed: 9262496]
20. Lo Coco F, Gaidano G, Louie DC, Offit K, Chaganti RS, Dalla-Favera R. p53 mutations are associated with histologic transformation of follicular lymphoma. Blood 1993;82:2289–95. [PubMed: 8400281]
21. Sander CA, Yano T, Clark HM, et al. p53 mutation is associated with progression in follicular lymphomas. Blood 1993;82:1994–2004. [PubMed: 8400252]
22. Davies AJ, Lee AM, Taylor C, et al. A limited role for TP53 mutation in the transformation of follicular lymphoma to diffuse large B-cell lymphoma. Leukemia 2005;19:1459–65. [PubMed: 15902285]
23. Harvey M, McArthur MJ, Montgomery CA Jr. Butel JS, Bradley A, Donehower LA. Spontaneous and carcinogen-induced tumorigenesis in p53-deficient mice. Nat Genet 1993;5:225–9. [PubMed: 8275085]
24. Ward JM, Tadesse-Heath L, Perkins SN, Chattopadhyay SK, Hursting SD, Morse HC III. Splenic marginal zone B-cell and thymic T-cell lymphomas in p53-deficient mice. Lab Invest 1999;79:3–14. [PubMed: 9952106]
25. Jacks T, Remington L, Williams BO, et al. Tumor spectrum analysis in p53-mutant mice. Curr Biol 1994;4:1–7. [PubMed: 7922305]
26. Wang P, Lushnikova T, Odvody J, Greiner TC, Jones SN, Eischen CM. Elevated Mdm2 expression induces chromosomal instability and confers a survival and growth advantage to B cells. Oncogene 2007;27:1590–8. [PubMed: 17828300]
27. Coles AH, Liang H, Zhu Z, et al. Deletion of p37Ing1 in mice reveals a p53-independent role for Ing1 in the suppression of cell proliferation, apoptosis, and tumor-igenesis. Cancer Res 2007;67:2054–61. [PubMed: 17332334]
28. Kichina JV, Zeremski M, Aris L, et al. Targeted disruption of the mouse ing1 locus results in reduced body size, hypersensitivity to radiation and elevated incidence of lymphomas. Oncogene 2006;25:857–66. [PubMed: 16170338]

29. Campos EI, Chin MY, Kuo WH, Li G. Biological functions of the ING family tumor suppressors. Cell Mol Life Sci 2004;61:2597–613. [PubMed: 15526165]
30. Gong W, Suzuki K, Russell M, Riabowol K. Function of the ING family of PHD proteins in cancer. Int J Biochem Cell Biol 2005;37:1054–65. [PubMed: 15743678]
31. Nouman GS, Anderson JJ, Lunec J, Angus B. The role of the tumour suppressor p33 ING1b in human neoplasia. J Clin Pathol 2003;56:491–6. [PubMed: 12835293]
32. Soliman MA, Riabowol K. After a decade of study-ING, a PHD for a versatile family of proteins. Trends Biochem Sci 2007;32:509–19. [PubMed: 17949986]
33. Zeremski M, Hill JE, Kwek SS, et al. Structure and regulation of the mouse ing1 gene. Three alternative transcripts encode two phd finger proteins that have opposite effects on p53 function. J Biol Chem 1999;274:32172–81. [PubMed: 10542254]
34. Donehower LA, Harvey M, Slagle BL, et al. Mice deficient for p53 are developmentally normal but susceptible to spontaneous tumours. Nature 1992;356:215–21. [PubMed: 1552940]
35. Liang H, Chen Q, Coles AH, et al. Wnt5a inhibits B cell proliferation and functions as a tumor suppressor in hematopoietic tissue. Cancer Cell 2003;4:349–60. [PubMed: 14667502]
36. Egle A, Harris AW, Bouillet P, Cory S. Bim is a suppressor of Myc-induced mouse B cell leukemia. Proc Natl Acad Sci U S A 2004;101:6164–9. [PubMed: 15079075]
37. Marfella CG, Ohkawa Y, Coles AH, Garlick DS, Jones SN, Imbalzano AN. Mutation of the SNF2 family member Chd2 affects mouse development and survival. J Cell Physiol 2006;209:162–71. [PubMed: 16810678]
38. Jones SN, Roe AE, Donehower LA, Bradley A. Rescue of embryonic lethality in Mdm2-deficient mice by absence of p53. Nature 1995;378:206–8. [PubMed: 7477327]
39. de Jong D. Molecular pathogenesis of follicular lymphoma: a cross talk of genetic and immunologic factors. J Clin Oncol 2005;23:6358–63. [PubMed: 16155020]
40. Pasqualucci L, Neumeister P, Goossens T, et al. Hypermutation of multiple proto-oncogenes in B-cell diffuse large-cell lymphomas. Nature 2001;412:341–6. [PubMed: 11460166]
41. Phan RT, Dalla-Favera R. The BCL6 proto-oncogene suppresses p53 expression in germinal-centre B cells. Nature 2004;432:635–9. [PubMed: 15577913]
42. Busslinger M. Transcriptional control of early B cell development. Annu Rev Immunol 2004;22:55–79. [PubMed: 15032574]
43. Bai M, Skyrlas A, Agnantis NJ, et al. B-cell differentiation, apoptosis and proliferation in diffuse large B-cell lymphomas. Anticancer Res 2005;25:347–62. [PubMed: 15816558]
44. Houldsworth J, Olshen AB, Cattoretti G, et al. Relationship between REL amplification, REL function, and clinical and biologic features in diffuse large B-cell lymphomas. Blood 2004;103:1862–8. [PubMed: 14615382]
45. Jost PJ, Ruland J. Aberrant NF-nB signaling in lymphoma: mechanisms, consequences, and therapeutic implications. Blood 2007;109:2700–7. [PubMed: 17119127]
46. Feng X, Bonni S, Riabowol K. HSP70 induction by ING proteins sensitizes cells to tumor necrosis factor alpha receptor-mediated apoptosis. Mol Cell Biol 2006;26:9244–55. [PubMed: 17030616]
47. Ohmori M, Nagai M, Tasaka T, et al. Decreased expression of p33ING1 mRNA in lymphoid malignancies. Am J Hematol 1999;62:118–9. [PubMed: 10577281]
48. Schraders M, Pfundt R, Straatman HM, et al. Novel chromosomal imbalances in mantle cell lymphoma detected by genome-wide array-based comparative genomic hybridization. Blood 2005;105:1686–93. [PubMed: 15498857]
49. Ripperger T, von Neuhoff N, Kamphues K, et al. Promoter methylation of PARG1, a novel candidate tumor suppressor gene in mantle-cell lymphomas. Haematologica 2007;92:460–8. [PubMed: 17488656]

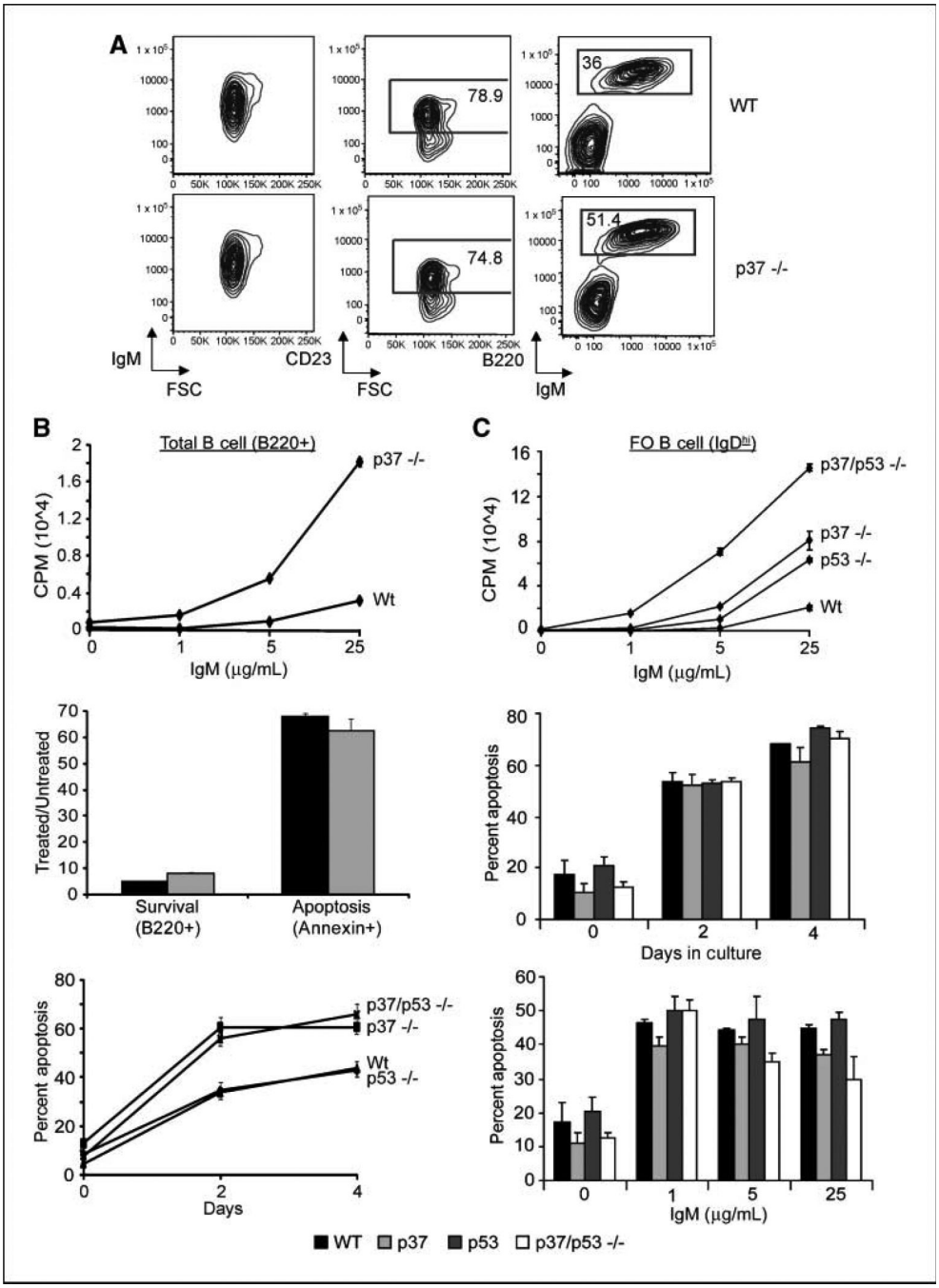

Figure 1.

Proliferation and apoptosis in p37-null and p37/p53-double null total B cells and FO B cells. *A*, FACS analysis of spleen cells from a healthy 8-mo-old wt control mouse and matched p37-null mouse. FSC is forward scatter (proportional to cell size). *Left and right plots*, all live spleen cells within the lymph scatter gate; *middle plots*, data from CD23+ B cells. *B*, [^{3}H] thymidine uptake assay of Wt, p53-null, p37-null, and p37/p53-double null purified total B cells (CD45R/B220+; *top*). Assay was performed in triplicate and repeated twice. B cells were treated with the indicated amount of anti-IgM and harvested 24 h for [^{3}H] thymidine uptake assay. *Middle*, mice were treated with 10Gy ionizing radiation and spleens were harvested 8 h later. Single cell suspensions were then stained with B220, Annexin V, and 7-AAD before being

analyzed by FACS. Shown is the ratio of treated versus untreated cells that were positive for B220 or Annexin V. Experiment was done in triplicate and repeated at least thrice. *Bottom*, apoptosis assay on purified total B cells (*B220+*) from Wt, p53-null, p37-null, and p37/p53-double null mice treated with 100 nmol/L dexamethasone. Plots show percent of sub-G_1. Assay was done in triplicate and repeated twice. *C*, [^{3}H] thymidine uptake assay of Wt, p53-null, p37-null, and p37/p53-double null–purified FO B cells (IgD^{hi}; *top*). Assay was done as in *B. Middle and bottom*, apoptosis assay on purified FO B cells (IgD^{hi}) from wt, p53-null, p37-null, and p37/p53-double null mice. FO B cells were either left in prolonged culture for 4 d, with cells being harvested and stained with propidium iodide every other day, or FO B cells were treated with increasing amounts of IgM and harvested 16 h later. Plots show percent of sub-G_1. Assays were done in triplicate and repeated twice.

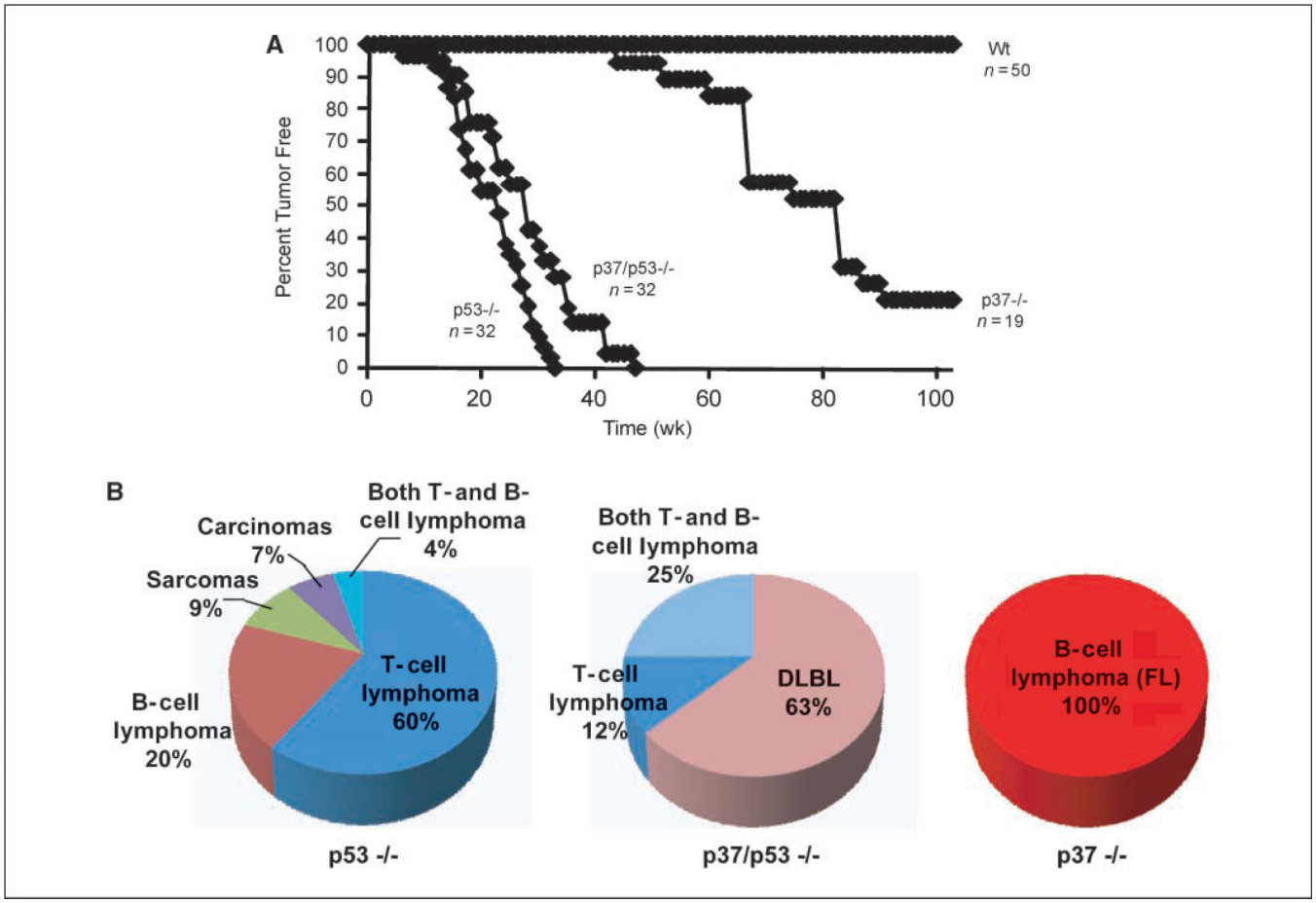

Figure 2.

Deletion of p53 alters the rate and spectrum of lymphomagenesis in p37-null mice. *A*, tumor curves of a cohort of mice that were deficient for p53, p37, or both tumor suppressors. Wt mice did not present with tumors during this time period. *B*, relative percentage of different tumor types arising spontaneously in p53-null, p37/p53-double null, and p37-null mice. Whereas 100% of tumors arising in p37-null mice were classified as FL, a majority of the tumors present in p37-null mice codeleted for p53 were DLBL. No tumors other than lymphomas were present in p37/p53-double null mice.

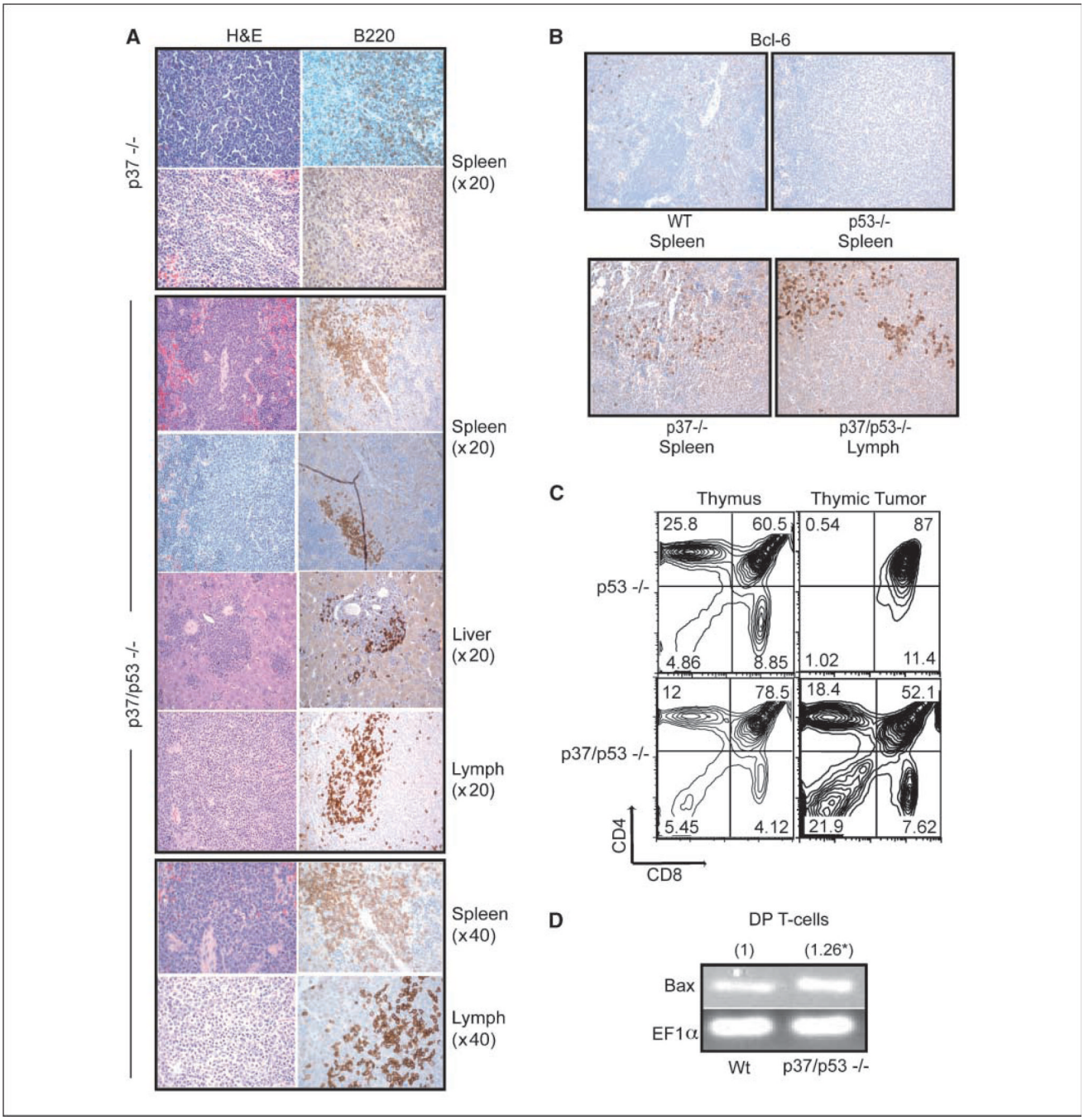

Figure 3.

Characterization of tumors from p37/p53-double null mice. *A*, representative H&E or CD45R/B220-stained tumor sections from p37-null or p37/p53-double null mice. The p37/p53-double null liver, lymph node, and first spleen sections are from one mouse. All pictures were taken at ×20 magnification unless otherwise indicated. *B*, representative Bcl-6 stained wt, p53-null, p37-null, and p37/p53-double null spleenic or lymph node tumors. All pictures were taken at ×20 magnification. *C*, FACS plot of CD4 and CD8-stained thymic tumors from p53-null or p37/p53-double null mice. *D*, relative fold induction of *Bax* expression by quantitative real-time RT-PCR on CD4/CD8 DP sorted T cells from wt or p37/p53-double null thymii.

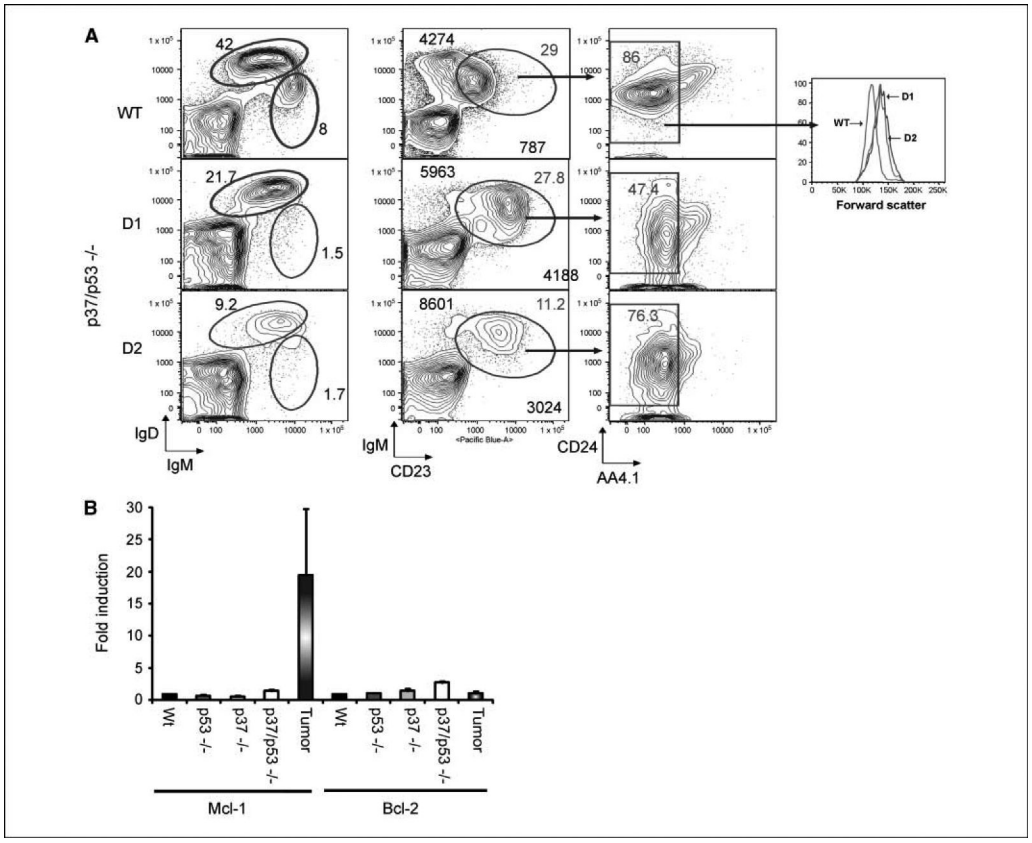

Figure 4.

Tumors from p37/p53-double null mice are derived from FO B cells and have elevated *Mcl-1* expression. *A*, representative FACS analysis of spleen cells from a healthy wt control mouse (*WT*) and spleen cells from two different p37/p53-double null mice with tumors (*D1* and *D2*). *Middle column*, the larger bold numbers report the geometric mean fluorescence intensity values for IgM (*y* axis) and CD23 (*x* axis) for the $IgM^{+}CD23^{+}CD24^{+/-}AA4.1^{-}$ population. This experiment was repeated with similar results. *B*, expression levels of *Bcl-2* and *Mcl-1* assayed by quantitative real-time RT-PCR in spleens from wt, p53-null, p37-null, and p37/p53-double null mice or on p37/p53-double null splenic tumors. Real-time PCR of normal spleens was done in triplicate; *columns*, mean of tumor samples from three independent mouse tumors; *bars*, SD.

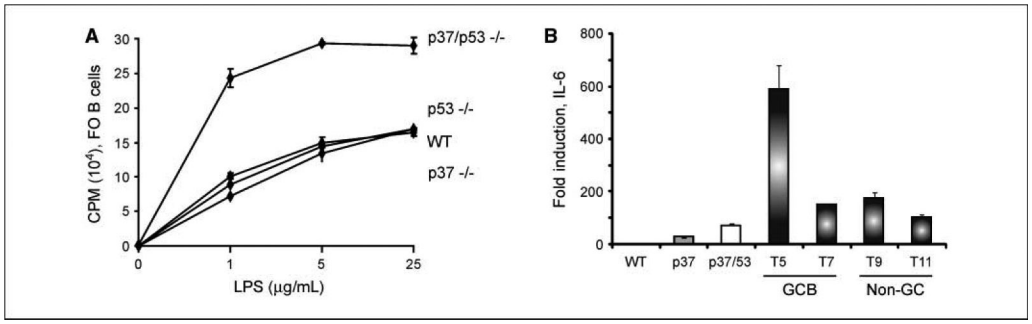

Figure 5.

FO B cells from p37/p53-double null mice show elevated NF-κB activity. *A*, [^{3}H] thymidine uptake assay of Wt, p53-null, p37-null, and p37/p53-double null purified FO B cells (IgD^{Hi}). Assay was done in triplicate and repeated twice. B cells were treated with the indicated amount of LPS and harvested 24 h later for [^{3}H] thymidine uptake assay. *B*, relative fold induction of *IL-6* in Wt, p37-null, p37/p53-double null spleens, and representative p37/p53-double null GCB (n = 2) and non–GC-DLBL (n = 2) tumors by quantitative real-time RT-PCR. *Columns*, mean of quantitative real-time RT-PCR performed in triplicate; *bars*, SD.

Table 1

Expression of DLBL markers (fold induction)

Tumor	CD10	Bcl-6	lrf-4	Classification	RelA
T1	—	27.7	GCB	72.6	
T2	—	—	—	Non-GC	73.9
T3	—	—	—	Non-GC	4.5
T4	2.3	—	—	GCB	2.5
T5	306.4	—	—	GCB	10.4
T6	—	12.5	—	GCB	4.2
T7	—	86.9	—	GCB	21.5
T8	—	—	—	Non-GC	—
T9	—	13.2	—	GCB	31.5
T10	6.7	29.6	—	GCB	53.5
T11	—	—	—	Non-GC	6.8
T12	—	—	—	Non-GC	—
T13	—	3.6	—	GCB	3.3

NOTE: p37/p53-double null mice develop predominately GCB DLBL and have elevated *RelA* expression and activity. Table shows classification of 13 independent p37/p53-double null spleenic tumors based on relative fold induction of *CD10*, *lrf-4*, and *Bcl-6* by quantitative real-time RT-PCR. Also shown is the relative fold induction of *p65/RelA* in the same 13 spleenic tumor samples. Values are averages of relative fold induction of three independent experiments for each tumor. SDs were within 10% of the mean value for each sample.